Rare Metal Materials and Engineering
Volume 45, Issue 12, December 2016
Online English edition of the Chinese language journal

Available online at www.sciencedirect.com
ScienceDirect

Cite this article as: Rare Metal Materials and Engineering, 2016, 45(12): 3050-3056.

ARTICLE

Surface Morphology and Affected Layer in Disc-milling Grooving of Titanium Alloy

Xin Hongmin, Shi Yaoyao

Key Laboratory of Contemporary Design and Integrated Manufacturing Technology, Ministry of Education, Northwestern Polytechnical University, Xi'an 710072, China

Abstract: Disc-milling grooving experiment was carried out to measure milling force and temperature for titanium alloy samples. After machining, surface roughness, surface topography, residual stress, microstructure and microhardness under different milling conditions were analyzed. The results show that the surface roughness of the center on milling surface is lower than that of the edge; moreover, the surface roughness decreases with the increase of the spindle speed, but increases with the increase of depth of cut and feed speed. The residual compressive stress is produced on the machined surface and subsurface, and gradually declines to zero with increase of the depth. The microstructure of lattice tensile deformation is found along feed direction under the effect of milling force, progressing from the initial equiaxed structure to long flake lattice. The metallographic structure of plastic deformation zone changes with the temperature, transforming from the initial equiaxed microstructure to a lamellar microstructure when the temperature is up to β-phase transition temperature. The combination of mechanical and thermal loads increases the microhardness on the machined surface and subsurface.

Key words: titanium alloy; disc-milling; surface roughness; surface topography; microhardness; microstructure

The titanium alloy is widely used in aerospace, aviation, navigation, automobile and other industries because of its advantages like small density, high intensity, high temperature resistance and good corrosion resistance [1]. However, the machining quality and efficiency are limited by the unique characteristics of titanium alloy like low thermal conductivity, small elastic modulus and high chemical activity, which can bring a high cutting temperature, great cutting force and a small distortion coefficient. Meanwhile the sticking phenomenon and tool wear are severe in the process of machining [2]. Noticeable changes happen in the microstructure and microhardness on the machined surface in high speed milling titanium alloy. Serious plastic deformation and work hardening are observed when improper cutting factors are employed, leading to adverse effects on fatigue life of materials [2,3].

Recently, multitude researches were conducted on the surface integrity for high speed milling titanium alloy. A large number of experiments show that small residual stress and a hardened layer can be obtained by high speed milling of titanium alloy [4,5]. Du et al.[6] studied the surface morphology and microstructure of TC4 titanium alloy under high-speed milling. The results showed that the milling surface quality becomes better with increasing the spindle speed. Yang et al.[7] researched the effect of high-speed milling parameters on surface integrity of TC4 titanium alloy. The results showed that the effect of spindle speed on surface roughness, surface topography and microhardness is obvious, and the effect of axial cutting depth on surface roughness, surface topography is remarkable. Yang et al.[8] carried out two-dimensional simulation of TC4 titanium alloy in the high-speed milling process. They found that the highest temperature in the cutting zone locates on tool chip interface at a distance of 0.01~0.02 mm from the tool tip.

Received date: December 28, 2015
Foundation item: National Numerical Control Major Projects Foundation of China (2013ZX04001081); National Natural Science Foundation of China (50975237, 51005184); Aerospace Research Foundation of China (2013ZE53060)
Corresponding author: Xin Hongmin, Candidate for Ph. D., Key Laboratory of Contemporary Design and Integrated Manufacturing Technology, Ministry of Education, Northwestern Polytechnical University, Xi'an 710072, P. R. China, Tel: 0086-29-88493232-244, E-mail: xhm0330@163.com

The influence of the milling speed on the cutting temperature is significant. Sridhar et al.[9] focused on the effect of machining parameters and heat treatment on the residual stress in titanium alloy IMI-834. The residual compressive stresses are found to be dependent upon the milling parameters. Yao et al.[10] researched residual stress in high speed milling of titanium TC11 alloy under different cooling conditions, tool rake angles and milling parameters. The results showed that emulsion cooling gets the highest surface residual compressive stress and the dry cutting gets the lowest. With the increase of cutting tool rake angle, surface residual compressive stress increases. Daymi et al.[11] investigated the effect of machining condition on surface integrity of TC4 alloy using a high speed ball end milling process with various milling parameters, in a dry condition on a vertical five-axis CNC machine. Wu et al.[12] studied the formation mechanism and influence of cutting parameters on residual stress in flank milling of TB6 through orthogonal experiments. Experiments result showed that the cutting temperature varies between 300 and 518 ℃, while residual compressive stress on the machined surface is from –199.8 MPa to –41.7 MPa. Residual tensile stress occurs on subsurface with increasing milling parameters excessively. Yang et al.[13] focused on the machined surface integrity of TC11 titanium alloy under different cutting conditions. It is shown that surface residual stress is compressive, and decreases with increasing the milling speed in both feed and stepover directions. When the milling speed increases, surface roughness increases obviously. The microstructure of surface layer does not change obviously. Daymi et al.[14] researched surface integrity in high speed end milling of TC4 under dry condition. The machined surface roughness, residual stress, microhardness and microstructure were observed.

Some research of cutting types like end milling and face milling has been carried out to study the surface integrity in high speed milling titanium alloy. Based on the best of our knowledge, few studies have been dedicated to disc milling at low speed, especially research on the thermal-mechanical coupling effect on surface morphology and the affected layer. Disc milling is widely used in machining for its capability to provide large cutting force and high milling efficiency. It is quite a new method applied in large-size blade and blisk machining. The grooving efficiency for blisk is greatly improved using a disc milling approach verified by experiments. However, the problem of deeper plastic deformation layers caused by big milling force and high temperature, which has a significant influence on fatigue life of parts, is not studied yet.

Therefore, the disc milling grooving was studied in the present research, and the surface morphology and the affected layer were focused on. First, the milling force and temperature were measured. Based on the results, the thermal-mechanical coupling effect on surface roughness, surface topography, residual stress, microstructure and microhardness was analyzed to study the formation mechanism of surface morphology and the affected layer. The results provide the experimental basis for technological parameter optimization and controlling the surface integrity of disc milling grooving for blisk.

1 Experiment

Titanium alloy (Ti6Al4V) was chosen as the experiment material in the present study, which is one kind of $\alpha + \beta$ phase titanium alloy. It has many advanced properties such as comprehensive mechanics performance, great specific strength and low thermal conductivity which extend its application in aviation. The main chemical composition and mechanical properties are shown in Table 1 and Table 2, respectively. The tested hardness of material is 33~35 HR.

XH716 VMC was used as the milling machine, staggered teeth disc cutter with three edges was applied for climb milling under wet cutting condition. The parameters of the disc cutter are shown in Table 3. In order to obtain the milling force and temperature in different milling parameters (spindle speed, depth of cut and feed speed), the specific processing parameters of disc milling are shown in Table 4.

Milling temperature was measured by a semi-artificial thermocouple composed of TC4 alloy (φ 0.03 mm) and constantan (φ 0.03 mm). Milling force was tested in three directions of *x*, *y* and *z* by a dynamic piezoelectric dynamometer. The wave of milling force was recorded by DEWESOFT. Milling temperature and milling force would provide a theory basis to the alternation of machined surface. Measurement results are shown in Table 4. The milling schematic diagram is shown in Fig.1.

TR240 rough meter was applied to measure surface roughness. Five points were chosen along the milling direction on milling surface, and surface roughness of each point was measured to acquire R_{a1}, R_{a2}, R_{a3}, R_{a4} and R_{a5}. Sampling length of measuring was 0.8 mm and assessment was 5.6 mm. Then these five values were averaged.

The three-dimensional surface topography was detected by optical VECOO 3D surface topography tester NT100. The surface morphology was measured by QUANTA 200 scanning electron microscope (SEM) in a secondary electron (SE) mode.

The microstructure was observed by metallurgical optical microscope S6D. In this step, the sample was firstly cut along the affected layer direction to make the embedded samples, and then the embedded samples were ground and polished with a metallographic grinder. Before observation, the embedded samples were etched for 5~10 s using a corrodent matched by $HF : HNO_3 : H_2O = 1 : 1 : 20$.

Table 1 Chemical composition of TC4 alloy (wt%)

Al	V	Fe	C	O	H	N
5.50~6.75	3.50~4.50	0.3	0.1	0.2	0.015	0.05

Table 2 Mechanical properties of TC4 at room temperature

σ_b/MPa	$\sigma_{r0.2}$/MPa	δ/%	ψ/%
≥895	≥825	≥10	≥25

Table 3 Parameters of disc cutter

Diameter/mm	Number of teeth	Thickness/mm	Body material	Blade material	Rake angle/(°)	Relief angle/(°)	Inclination angle/(°)	Auxiliary angle/(°)
200	16	20	Structural alloy steel	YG6	5	4	15	20

Table 4 Experiment parameters and results for samples

Samples No.	n/r·min^{-1}	a_p/mm	v_f/mm·min^{-1}	F_x/N	F_y/N	F_z/N	T/℃
1#	40	6	70	1425	1240	1137	532
2#	55	6	70	1320	1053	992	607
3#	70	6	70	1215	966	857	774
4#	85	6	70	1110	917	721	824
5#	100	6	70	926	809	553	1024
6#	70	2	70	836	742	512	604
7#	70	4	70	963	831	587	661
8#	70	6	70	1215	966	857	774
9#	70	8	70	1657	1415	834	743
10#	70	10	70	2033	1906	1197	812
11#	70	6	40	986	763	613	570
12#	70	6	55	1034	865	679	645
13#	70	6	70	1215	966	857	774
14#	70	6	85	1341	1126	976	849
15#	70	6	100	1466	1227	1078	967

Microhardness at different depths below the surface was measured with 600MRD digital display type hardness tester. First, the embedded samples were made, and then the embedded samples were ground and polished with a metallographic grinder. Finally, with a Vicker indenter, the applied load was 25 g and the dwell time was 6 s on the cross section of embedded samples from a depth of 10~20 μm point by point. For each sample, three points were undertaken at the same depth but spaced to avoid interference. Average value of three measurement results was considered for analysis.

The surface residual stresses were evaluated using the ψ tilt X-ray method by an XS tress 3000 with Cu Kα radiation. The residual stress distribution on milling layer was measured with electrochemical corrosion. The specific operation method was as follows: the machined surface is stripped with electropolisher, and the stripped depth is controlled by controlling electrolytic time. The change of depthwas measured with the micrometer. For the samples stripped, the residual stress was tested until close to the body material's residual stress.

2 Results and Discussion

2.1 Surface roughness

Milling schematic diagram is shown in Fig.1. Two points of A (center of machined surface) and B (edge of machined surface) were selected to measure surface roughness. The effects of the milling parameters on surface roughness are compared in Fig.2. It can be seen from Fig.2 that the surface roughness decreases with the increasing spindle speed, but increases with the increasing depth of cut and the feed speed.

It is widely known that the surface quality is determined by milling force and milling heat transferring to the machined surface. Therefore, the results displayed by Fig.2 can be explained that, first, the milling temperature increases with the increasing spindle speed, and the increasing milling temperature decreases the material's elastic deformation coefficient and friction coefficient. Then, milling force declines and the milling process becomes stable, so the surface roughness decreases. Second, although milling heat increases with the increasing spindle speed, most of milling heat is taken away with cuttings when the spindle speed increases ceaselessly, while only a small amount of milling heat is transferred to the machined surface, so the temperature of machined surface is not high, and less surface defects and low surface roughness can be obtained. For the milling parameters of depth of cut and feed

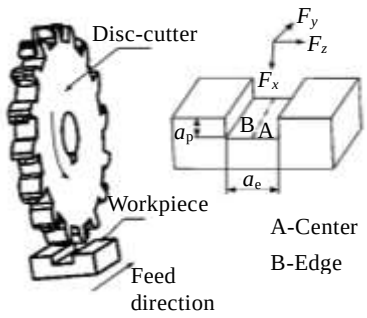

F_x-milling force in x-direction, F_y-milling force in y-direction, F_z-milling force in z-direction, a_p-depth of cut, a_e- width of cut

Fig.1 Milling schematic diagram

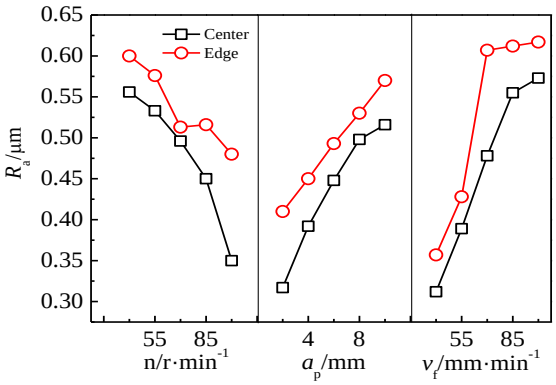

Fig.2 Effects of milling parameters on surface roughness

speed, cutting thickness and cutting areas increase with increase in them, which induces bigger milling force and tool vibration. The instability of machining process will increase surface plastic deformation, so the surface roughness increases. In addition, the milling temperature increases with increasing depth of cut and feed speed, the range of milling temperature is from 532 ℃ to 1024 ℃ in this milling parameter range of the present study (exceeding the β-phase transition temperature of 1005 ℃). Such a high milling temperature may cause plastic deformation on the machined surface, so the surface flaw is produced, and the surface roughness increases.

Fig.2 indicates that the surface roughness of the center is lower than that of the edge. It is due to that most of the milling heat of the center is taken away by cuttings, but the milling heat of the edge is transferred to the workpiece, so the surface quality is easily improved at the center of the machined surface.

2.2 Surface topography

The three-dimensional surface topography and SEM images of surface are shown in Fig.3 and Fig.4, with the same milling parameters, including spindle speed n=100 r/min, a_p=6 mm, and feed speed v_f = 70 mm/min. Fig.3 shows that the milling surface topography of the center is smooth, and the gap and scratch is not obvious. However, the scratch of the edge is obvious, and the milling texture is clearly visible (Fig.4). The surface roughness of the center is 0.312 μm, the maximum height of peak and ditch of milling surface are 1.58 and 1.49 μm, respectively. The surface roughness of the edge is 0.435 μm, the maximum height of peak and ditch of milling surface are 2.1 and 2.56 μm, respectively. The observation result of surface topography is consistent with the measurement.

It can be explained as follows: first, the milling force experiment in the present study indicates that F_x is the biggest, F_y is smaller than F_x, the last one is F_z. Therefore, the pressure of main cutting edge (near the center of milling surface) is biggest, and the contact between the tool and the workpiece is stable, so the surface quality of the center is relatively good. However, the pressure of tool tip radius (near the edge of milling surface) is smaller than the pressure of the main cutting edge, which intensifies the instabilities and tool wear in machining process, and thus the surface quality of the edge is poor. In addition, most of cutting heat, near the main cutting edge, is taken away by cuttings. Whereas, the cutting heat near tool tip radius is almost transferred to the workpiece, so the temperature of the edge is higher than that of the center. This is one of the reasons why the surface quality of the edge is poor.

2.3 Residual stress

The samples machined with milling parameters of samples 5#, 10# and 15# are selected to study the residual stress distribution. The residual stress distribution law curves are shown in Fig.5. The curves indicate that residual compressive stress appears on the milling surface and the subsurface, and gradually approximates to zero with the increase of h (h represents the depth below surface). The values of residual stress on machined surface of samples 5#, 10# and 15# are −449.72, −598.01 and −414.2 MPa, respectively. The depth of residual stress layer h_s for samples 5#, 10# and 15# are about 270, 280, and 210 μm, respectively. Therefore, it can be concluded that the bigger residual stress on machined surface, the deeper the depth of residual stress layer.

The results can be explained as follows: on one hand, the force of disc-milling is large, which revealed in x direction of samples 5#, 10# and 15# are 926, 2033 and 1466 N, respectively; as a result, the friction and squeezing occur between the cutting tool flank and the workpiece upon the skin layer, and severe plastic deformation appears. In the plastic deformation zone, the specific volume of the skin layer metal increases and the volume expands, while the inner layer metal prevents the transformation. Because the skin layer metal is limited by the inner layer metal, the residual compressive stress is generated on the skin layer metal. On the other hand, high temperature can be reached in the milling zone since Ti-6Al-4V alloy has low thermal

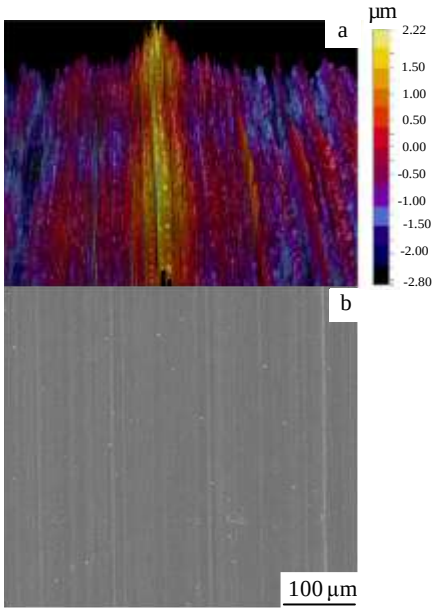

Fig.3 Milling three-dimensional surface topography (a) and SEM image (b) of the center surface

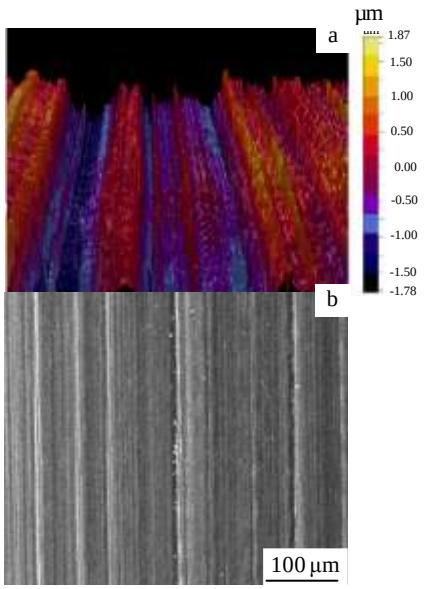

Fig.4 Milling three-dimensional surface topography (a) and SEM image (b) of the edge

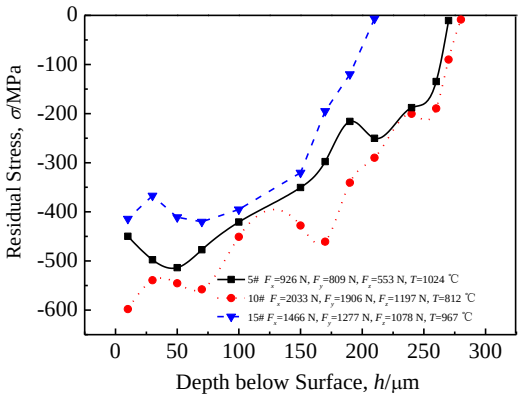

Fig.5 Distribution of residual stress on subsurface

conductivity. At the same time, the contact length between the chip and the rake face is short, and the milling heat is difficult to release. As a result, the microstructure of skin layer metal is changed and the volume expands, generating residual compressive stress.

2.4 Microstructure and microhardness

Fig.6 shows the microstructure and microhardness of sample 5#. F_x, F_y and F_z are 926, 809 and 553 N respectively. Milling temperature is 1024 ℃, which exceeds the β-phase transition temperature (1005 ℃), and will alter the extensive metallographic structure. In Fig.6a, the limited amount of α-phase is left and the β-phase is precipitated after quickly cooling, causing the initial equiaxed micro structure to almost change into a lamellar microstructure. The tensile deformation is not obvious. The depth of deformation layer h_M is about 113 μm.

Fig.6b is the variation curve of microhardness of sample 5#. The surface hardness parameter is 47.89 HR, and the hardened degree is about 36%. The hardness parameter gradually approximates to the body hardness parameter. The depth of hardened layer h_H is about 150 μm. The variation curve of microhardness just validates the alteration of microstructure. Because the α-phase fully changes into the lamellar microstructure under the effect of higher milling temperature, thanks to the lamellar microstructure has advantage of high strength and fracture toughness, but low tensile plasticity and fatigue strength, thus leads to the enhanced surface hardness. For sample 5#, the milling temperature plays a leading role on the affected layer.

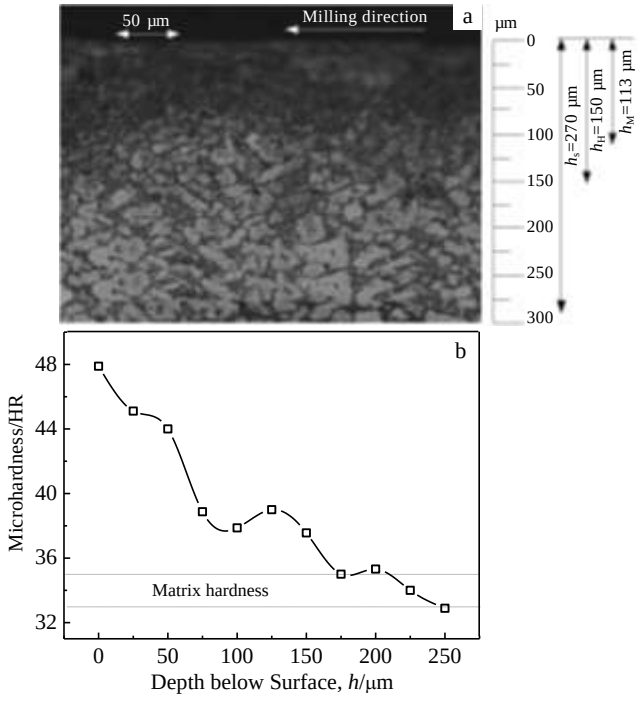

Fig.6 Microstructure (a) and microhardness (b) of sample 5#

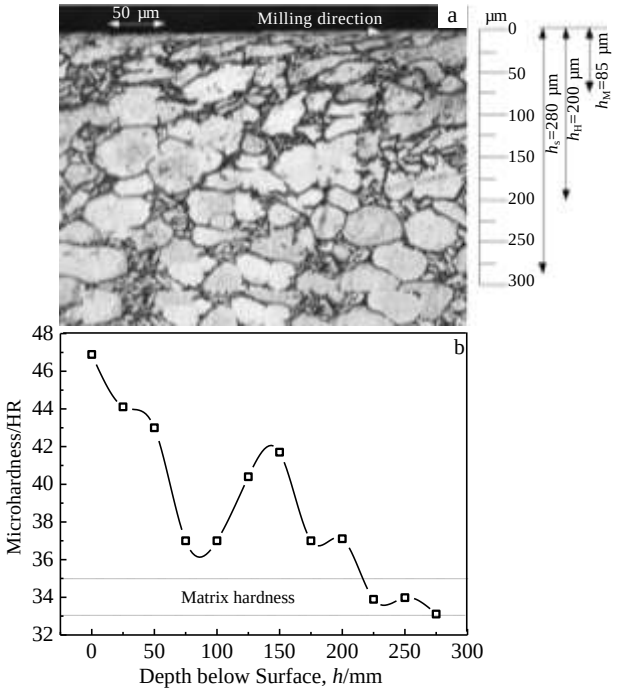

Fig.7 Microstructure (a) and microhardness (b) of sample 10#

Fig.7 shows the microstructure and microhardness of sample 10#. F_x, F_y and F_z are 2033, 1906 and 1197 N, respectively. The plastic deformation is obvious on the milling surface seen from Fig.7a. The lattice tensile deformation along the feed direction is observed, caused by milling force. The α-phase progresses from the initial equiaxed structure to the long flake lattice. The depth of deformation layer h_M is about 85 μm. Because the milling temperature reaches 812 ℃, which is not up to the β-phase transition temperature (1005 ℃), the phase transition is not observed.

The variation curve of microhardness of sample 10# as a function of distance below the machined surface is plotted in Fig.7b. The surface hardness parameter is 46.89 HR, and the hardened degree is about 33%. The hardness parameter gradually declines to 37.15 HR beneath the machined surface 0~100 μm, then increases to 41.77 HR beneath the machined surface 125~150 μm, and finally approximates to the body hardness parameter. The depth of hardened layer h_H is about 200 μm. The variation curve of microhardness just proves the alteration of microstructure. Obvious plastic deformation appears on the machined surface, which increases material's surface hardness. Since the phase transition is not observed, the milling force has a significant effect on the affected so layer relative to milling temperature for sample 10#.

Fig.7 also displays that the residual stress irregularly changes with the increasing milling temperature and force, because the residual stress is a combined effect of milling temperature and force. The combined effect determines the distribution of residual stress. Although the depth of residual stress seems large, the residual compressive stress is profitable to improve fatigue life of parts.

Fig.8 shows the microstructure and microhardness of sample 15#. F_x, F_y and F_z are 1466, 1227 and 1078 N, respectively. It can be seen from Fig.8a that the plastic deformation is obvious on the machined surface, induced by the combined effect of cutting elastic and plastic deformation, the friction between the tool and cuttings, the friction between the tool and the machined surface. The lattice tensile deformation is also observed along the feed direction. Although the alteration of microstructure is similar to that of sample 10#, the distortion of α-phase is less obvious than that of that of sample 10#. This is because the milling force of sample 15# is smaller than sample 10#. The depth of deformation layer h_M is about 75 μm, which is also not deeper than that of sample 10#. 967 ℃ is recorded in experiment of sample 15#, which is close to the β-phase transition temperature (1005 ℃), but not up to it, so the phase transition isn't produced.

Fig.8b displays the variation curve of microhardness of sample 15#. The surface hardness parameter is 44.73 HR, and the hardened degree is ~32%. The hardness parameter gradually declines beneath the machined surface 0~75 μm, then increases beneath the machined surface 100 μm, afterwards approximates to body hardness parameter 33~35 HR. The depth of the hardened layer h_H is about 175 μm. The variation curve of microhardness just demonstrates the alteration of microstructure. The plastic deformation layer

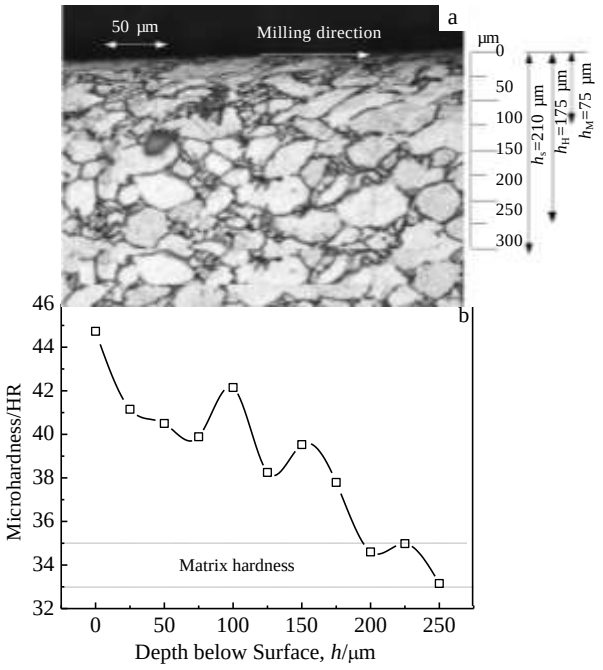

Fig.8 Microstructure (a) and microhardness (b) of sample 15#

on machined surface with the lattice distortion under milling force increases material's hardness. Likewise, milling force has an impact on the affected layer for sample 15#.

From the above analyses, it is illustrated that milling heat and milling force both have a significant influence on micro-structure and microhardness. Lattice tensile deformation is produced on the machined surface caused by milling force along the feed direction, and with greater milling force, more tensile deformation is generated. The metallographic structure of the plastic deformation zone changes with the temperature. Based on the effects above, a hardened layer appears and raises the hardness of plastic deformation zone.

3 Conclusions

1) Surface roughness value decreases with the increasing spindle speed, but increases with the increase of depth of cut and feed speed. The surface topography of the center on milling surface is smooth, and the gap is not obvious. The scratch of the edge on milling surface is obvious, and the milling texture is clearly visible.

2) The residual compressive stress is found on the machined surface and subsurface, gradually declines with the increase of *h*. The depth of residual stress layer are 270, 280 and 210 μm for sample 5#, 10# and 15#, respectively.

3) Lattice tensile deformation is produced on the machined surface caused by milling force along the feed direction. The metallographic structure of the plastic deformation zone changes with the temperature. Based on the effects above, a harden layer appears and raises the hardness of plastic deformation zone.

References

1 Mhamdi M B, Boujelbence M, Bayraktar E *et al*. *Physics Procedia*[J], 2012, 25(22): 355

2 Che-Haron C H. *Journal of Materials Processing Technology* [J], 2001, 118(1-3): 231

3 Che-Haron C H, Jawaid A. *Journal of Materials Processing Technology*[J], 2005, 166(2): 188

4 Ge Y F, Fu Y C, Xu J H. *Key Eng Mater*[J], 2007, 339: 6

5 Wang F Z, Zhao J, Li A H *et al*. *Mach Sci Tech*[J], 2014, 18(3): 448

6 Du Suigeng, Lv Chao, Ren Junxue *et al*. *Acta Aeronautica et Astronautica Sinica*[J], 2008, 30(6): 1710 (in Chinese)

7 Yang Z C, Zhang D H, Yao C F *et al*. *Journal of Northwestern Ploytechnical University*[J], 2009, 27(4): 538 (in Chinese)

8 Yang Z C, Zhang D H, Yao C F *et al*. *Journal of Nanjing University Aeronautics Astronautics*[J], 2009, 41(5): 644 (in Chinese)

9 Sridhar B R, Devananda G, Ramachandra K *et al*. *Journal of Materials Processing Technology*[J], 2003, 139(1-3): 628

10 Yao Changfeng, Yang Zhenchao, Huang Xinchun *et al*. *Advanced Materials Research*[J], 2012, 443-444: 160

11 Daymi A, Boujelbene M, Bayraktar E *et al*. *Advanced Materials Research*[J], 2011, 264-265: 1228

12 Wu D X, Yao C F, Tian L *et al*. *Appl Mech Mater*[J], 2013, 328: 867

13 Yang Z C, Zhang D H, Yao C F *et al*. *2010 Inte conf Mech Auto Control Eng*[C]. Wuhan: MACE, 2010: 3334

14 Daymi A, Boujelbene M, Amara A B *et al*. *Mater Sci Technol* [J], 2010, 27(1): 387

盘铣开槽加工表面形貌与变质层研究

辛红敏, 史耀耀

(西北工业大学 现代设计与集成制造技术教育部重点实验室，陕西 西安 710072)

摘 要：设计盘铣开槽实验以测量盘铣切削钛合金时的切削力和切削温度，以切削力和切削温度实验为基础，分析不同切削条件下的表面粗糙度、表面形貌、残余应力、显微组织和显微硬度。结果表明：铣削表面中心处的粗糙度值小于边缘处，粗糙度值随着主轴转速的增加而减小，随着切削深度和进给速度的增加而增大。铣削表面和次表面均出现残余压应力，随着深度的增加，残余压应力逐渐减小为零。在切削力的作用下，晶粒沿进给方向发生明显的拉伸变形，α 相从初始等轴态拉伸为长片状。随着切削温度的升高，塑性变形区的金相组织发生改变，当切削温度达到 β 相转变温度时，金相组织从初始等轴态转变为全片层组织。热力耦合作用使得已加工表面和次表面硬度值升高。

关键词：钛合金；盘铣；粗糙度；表面形貌；显微硬度；微观组织

作者简介：辛红敏，女，1979 年生，博士生，西北工业大学现代设计与集成制造技术教育部重点实验室，陕西 西安 710072，E-mail: xhm0330@163.com